ELSEVIER

Polymer 43 (2002) 6515–6526

polymer

www.elsevier.com/locate/polymer

Mechanisms of ductile tear in blown film from blends of polyethylene and high melt strength polypropylene

A.C. Chang[a], S.P. Chum[b], A. Hiltner[a,*], E. Baer[a]

[a]*Department of Macromolecular Science, Center for Applied Polymer Research, Case Western Reserve University, Cleveland, OH 44106-7202, USA*
[b]*Polyolefins and Elastomers R&D, The Dow Chemical Company, Freeport, TX 77541, USA*

Received 29 April 2002; received in revised form 2 August 2002; accepted 5 August 2002

Abstract

Deformation processes associated with ductile tear in blown films of polyethylene blended with up to 30 wt% high melt strength polypropylene (hmsPP) were studied. The tear resistance was determined with a reinforced trouser tear test. During stable crack growth, a crack-tip damage zone was transformed into a continuous yielded zone at the fractured edge. The relationship to lamellar morphology was probed with atomic force microscopy. Balanced tear characteristics of polyethylene film reflected the nearly isotropic lamellar morphology. In contrast, the highly oriented shish-kebab morphology of hmsPP domains in the blend films resulted in increasingly anisotropic behavior as the amount of hmsPP increased. The most important manifestation was a significant reduction in machine direction (MD) tear. Good adhesion of polyethylene and hmsPP in blend films prevented interfacial failure and provided stress transfer to the dispersed phase at high strains. In MD tear, extension of the matrix by the normal processes of lamellar breakup and fibrillation caused rotation of hmsPP domains into the loading direction and in a later stage shear displacement of reoriented hmsPP lamellae. Locally, hmsPP domains constrained deformation of polyethylene lamellae. Factors that increased constraint on the polyethylene matrix such as increasing the amount of hmsPP or increasing the aspect ratio of hmsPP domains reduced the MD tear resistance. In transverse direction (TD) tear, the oriented hmsPP domains deformed by lamellar shear processes concurrently with lamellar breakup and fibrillation of the polyethylene matrix. As a result, the blend film preserved good TD tear resistance. © 2002 Published by Elsevier Science Ltd.

Keywords: Polyethylene; High melt strength polypropylene; Blown film

1. Introduction

Recent introduction of high melt strength polypropylene (hmsPP) with significantly enhanced melt processability makes it possible to realize the advantages of higher stiffness and higher heat resistance that polypropylene can bring to inherently tough and tear resistant polyethylene blown film [1,2]. The specific property balance depends on the oriented blend morphology achieved in the blown film process. A previous study that used primarily atomic force microscopy (AFM) and wide angle X-ray scattering (WAXS) methods to reveal the structure of blown film of linear low density polyethylene (LLDPE) blended with up to 30 wt% hmsPP showed that hmsPP was well-dispersed in the polyethylene matrix as thin elongated domains [3]. In the domains, hmsPP crystallized as planar row-nucleated structures with the long axis of the lamellae perpendicular to the extrusion direction. Row-nucleated hmsPP lamellae provided a template for epitaxial crystallization of polyethylene. The 42° angle of the lattice match imparted a characteristic herringbone texture to the polyethylene. Other researchers found that good adhesion of epitaxially crystallized polyethylene to polypropylene synergistically increased the mechanical properties of ultra-thin films [4–6].

Recognizing that a dispersed hmsPP phase might compromise the outstanding tear properties of polyethylene blown film a trouser tear test was developed specifically for evaluating tear resistance of thin ductile films [7]. The test differentiated among blown films of polyethylene blended with hmsPP on the basis of composition and thickness. Increasing the amount of hmsPP in the film decreased the tear resistance. Also, thinner films were less tear resistant than thicker films. The tear crack propagated with transformation of a crack-tip damage zone into a continuous yielded zone at the fractured edge. Formation of the damage

* Corresponding author. Tel.: +1-216-368-4186; fax: +1-216-368-6329.
E-mail address: pah6@po.cwru.edu (A. Hiltner).

0032-3861/02/$ - see front matter © 2002 Published by Elsevier Science Ltd.
PII: S0032-3861(02)00550-5

zone prevented mode III out-of-plane fracture. Instead, the film twisted 90° into the loading direction and failed in a tensile fracture mode. Correspondence in the energy to deform the material in the yielded zone and the measured tear energy demonstrated that yielding in the vicinity of the propagating crack provided the resistance to tearing in these films.

Introduction of a second phase into ductile polyethylene film reduced the amount of matrix yielding by constraining the structural changes that occurred during high strain deformation. Many studies over the years have contributed to the present understanding of structural changes during solid state deformation of polyethylene [8–12]. Although questions remain and investigations are ongoing, a general picture emerges in which the response to imposed strain begins with intralamellar shear along specific crystallographic planes and between crystal blocks in addition to interlamellar shear processes. At some point the lamellae lose their identity as they breakup into blocks that subsequently disintegrate and reform as fibrillar structures. The same concepts apply to tensile deformation of ductile LLDPE blown film [13]. Understanding the manner in which these processes are affected by a second phase is fundamental to strategies aimed at enhancing properties of polyethylene film through blending.

The present study employs primarily AFM to probe the plastic deformation processes that accompany ductile tearing of polyethylene film containing up to 30 wt% hmsPP. Interpretation of the results in terms of the previously elucidated hierarchical structure of the blend films forms the basis for understanding effects of composition, anisotropy and thickness on tear resistance of the films.

2. Materials and methods

2.1. Materials

A hmsPP, two LLDPEs, and blends of each of the polyethylenes with 10, 20 and 30 wt% of hmsPP were provided as blown film by The Dow Chemical Company. The films described in this, and previous studies [3,7], were processed in a Davis-Standard blown film line equipped with a 8.9 cm (3.5 in.) diameter extruder with a 30:1 length/diameter ratio and a 20.3 cm (8 in.) die. Melt temperature was set at 250 °C and the die gap was adjusted to 1.78 mm (70 mil). Blowup ratio was 2.5, and the frost line height was approximately 81 cm. Take-off rate was adjusted to produce 50 μm (2.0 mil) film and increased to produce 20 μm (0.8 mil) film.

As reported by the manufacturer, hmsPP was a modified impact resin with 16 wt% of an ethylene–propylene rubber (EPR) and melt flow index 0.35 g/10 min. One polyethylene was a Ziegler–Natta catalyzed ethylene–octene copolymer (znPE) with a density of 0.920 g cm^{-3} and a melt flow index of 1.0 g/10 min. The other polyethylene was a blend (zn/mPE) with a density of 0.916 g cm^{-3} that consisted of 63 wt% of a Ziegler–Natta catalyzed ethylene–octene copolymer ($\rho = 0.925$ g cm^{-3}) and 37 wt% of a metallocene catalyzed ethylene–octene copolymer ($\rho = 0.902$ g cm^{-3}), the blend had a melt flow index of 1.0 g/10 min. The melt flow index was measured with a load of 2.16 kg at 190 °C for polyethylene and at 230 °C for polypropylene. Additional characterization of the films was reported previously [3].

2.2. Methods

A reinforced trouser tear test previously developed for ductile films was used in this study [7]. Rectangular pieces with a width of 90 mm and a length of up to 60 cm were cut from the blown film with the long dimension parallel to extrusion to measure tear in the machine direction (MD) or perpendicular to extrusion to measure tear in the transverse direction (TD). For strain measurements, a grid pattern was applied to the center of the test area by inking through a square mesh with a 0.64 mm square grid. A notch about 3 cm in length was cut with a razor blade at one end of the test area. The notch produced two legs that were inserted into opposing grips in an Instron machine. To prevent stretching of the legs during testing a strip of 25 mm-wide fiber-reinforced tape was applied along the outer edge of each leg on opposite sides [7]. This left a test area 40 mm wide along the center of the strip. In the case of high tear resistance in the TD, the test area was increased to 50 mm to accommodate the larger amount of deformation.

The specimen was mounted in the Instron with reinforcing tape on the tension side of the legs. Extending the grips at 100 mm min^{-1} propagated the crack along the length of the reinforced tear specimen. Tear force was recorded against crosshead displacement. Tests were performed at ambient temperature or −10 °C in an environmental chamber and were typically repeated 4–6 times. During the tear test, a light source illuminated the strain markers from the back of the film and a video camera recorded deformation at the crack tip. After the tear test, the fractured film was pressed flat between two sheets of glass and the crack-tip damage zone was photographed in a light microscope between crossed polarizers.

To replicate the strain state ahead of the crack tip, the film was tested in constrained uniaxial tension in the direction perpendicular to crack growth. Specimens with gauge section 120 mm wide and 30 mm long were tested in an Instron machine. A 5 mm square grid pattern was used to measure strain. Crosshead speed was 100 mm min^{-1}.

To expose the lamellar morphology, films were etched with a 0.33 wt% solution of potassium permanganate in a 2:1 (v/v) mixture of concentrated sulfuric acid and 85% *ortho*-phosphoric acid [14]. Specimens were etched for about 1 h until the film thickness was reduced by about 10%.

Table 1
Tear properties of blown films

Material	hmsPP (wt%)	Density (g cm^{-3})	MD			TD		
			G_t (kJ m^{-2})	W (mm)	λ_c	G_t (kJ m^{-2})	W (mm)	λ_c
50 μm films								
hmsPP/znPE	0	0.9187 ± 0.0001	740 ± 30	19.1 ± 0.1	4.1 ± 0.1	700 ± 20	25 ± 1	5.6 ± 0.1
	10	0.9170	580 ± 50	14.6 ± 0.3	3.9 ± 0.3	670 ± 20	21 ± 1	4.7 ± 0.1
	20	0.9153	320 ± 50	5.7 ± 0.3	4.0 ± 0.3	690 ± 30	16 ± 2	4.8 ± 0.2
	30	0.9134	220 ± 20	4.8 ± 0.3	3.6 ± 0.2	‡	–	–
hmsPP/(zn/mPE)	0	0.9144 ± 0.0001	280 ± 10	8.3 ± 0.3	3.9 ± 0.1	320 ± 10	12 ± 1	3.8 ± 0.1
	10	0.9131	290 ± 30	7.0 ± 0.3	3.8 ± 0.1	290 ± 10	10 ± 1	4.0 ± 0.1
	20	0.9117	220 ± 20	5.1 ± 0.3	3.8 ± 0.2	310 ± 20	13 ± 1	3.6 ± 0.2
	30	0.9104	180 ± 10	3.8 ± 0.3	3.4 ± 0.1	‡	–	–
hmsPP	100	0.9019	34 ± 3	0.4 ± 0.1	–	230 ± 20	4 ± 1	2.7 ± 0.1
20 μm films								
hmsPP/znPE	0	0.9181 ± 0.0001	‡	–	5.8 ± 0.1	830 ± 40	27 ± 2	5.2 ± 0.2
	10	0.9157	210 ± 40	3.2 ± 0.3	4.0 ± 0.2	700 ± 30	21 ± 1	4.9 ± 0.3
	20	0.9135	120 ± 10	1.9 ± 0.3	4.2 ± 0.1	650 ± 40	18 ± 1	4.9 ± 0.2
	30	0.9115	90 ± 10	1.3 ± 0.3	3.9 ± 0.1	640 ± 50	23 ± 1	4.7 ± 0.1
hmsPP/(zn/mPE)	0	0.9125 ± 0.0001	‡	–	5.1 ± 0.1	350 ± 10	17 ± 2	3.9 ± 0.1
	10	0.9114	110 ± 10	2.5 ± 0.3	4.1 ± 0.1	310 ± 10	12 ± 1	3.4 ± 0.1
	20	0.9099	70 ± 10	1.9 ± 0.3	4.0 ± 0.1	320 ± 10	12 ± 1	3.5 ± 0.1
	30	0.9084	60 ± 10	1.3 ± 0.3	3.8 ± 0.1	360 ± 10	10 ± 1	3.2 ± 0.1
hmsPP	100	0.9014	20 ± 3	0.10 ± 0.05	–	310 ± 40	3 ± 1	2.9 ± 0.1

‡ represents curved crack path.

Light etching revealed the bulk morphology without damaging the delicate, deformed areas.

AFM images were obtained in air with a Digital Instruments Nanoscope IIIa fitted with a silicon tip operating in the tapping mode. Tapping at 50–70% of the free oscillation amplitude (A_o) with driving amplitude of 60–160 mV, considered to be moderately hard tapping, was used to bring out modulus differences between polypropylene and polyethylene while preserving textural differences.

3. Results and discussion

3.1. Tear energy

Initial loading in the trouser tear test produced a large damage zone at the crack tip that blunted the crack and prevented mode III out-of-plane fracture. Instead, the film twisted 90° into the direction of grip extension and failed in a tensile fracture mode. The tear crack propagated in a straight path at constant load in all trouser tear tests except for the MD tests of 20 μm films of znPE and zn/mPE and TD tests of 50 μm films with 30 wt% hmsPP. In these cases, the crack followed a curved trajectory until it encountered the reinforcing tape. Otherwise, the tear energy G_t was calculated from the load F and the film thickness t as $G_t = 2F/t$, Table 1. It was previously demonstrated that formation of the yielded zone provided the resistance to tearing in these films [7]. In this determination of G, the contribution of final separation was negligible.

In the MD, 50 μm films were more tear resistant than 20 μm films, increased hmsPP content reduced tear resistance, and films containing znPE were more tear resistant than films with zn/mPE, Fig. 1a. In contrast, TD tear energy did not depend on film thickness or on hmsPP content, Fig. 1b. All the films containing znPE had TD tear energy of roughly 700 kJ m^{-2}; films with zn/mPE had about half the tear energy. Indeed, higher tear resistance of films with znPE compared to films with zn/mPE was apparent in both MD and TD tear.

Comparing znPE and zn/mPE films, TD tear was about the same as MD tear of 50 μm films (MD tear of 20 μm films could not be measured due to the curved crack path). The balanced tear properties were consistent with the nearly isotropic lamellar morphology of znPE and zn/mPE films described previously [3]. At the other extreme, tear of hmsPP films was highly anisotropic exhibiting almost no tear resistance in the MD. The disparity in MD and TD tear reflected the highly oriented shish-kebab morphology of hmsPP film [3]. The blends exhibited gradually increasing anisotropy in tear properties as the amount of hmsPP increased. This was due primarily to a decrease in MD tear. The trend reflected the anisotropic blend morphology imparted by oriented hmsPP domains [3].

Crack propagation in a straight path left a plane stress yielded zone of constant width on either side of the fracture.

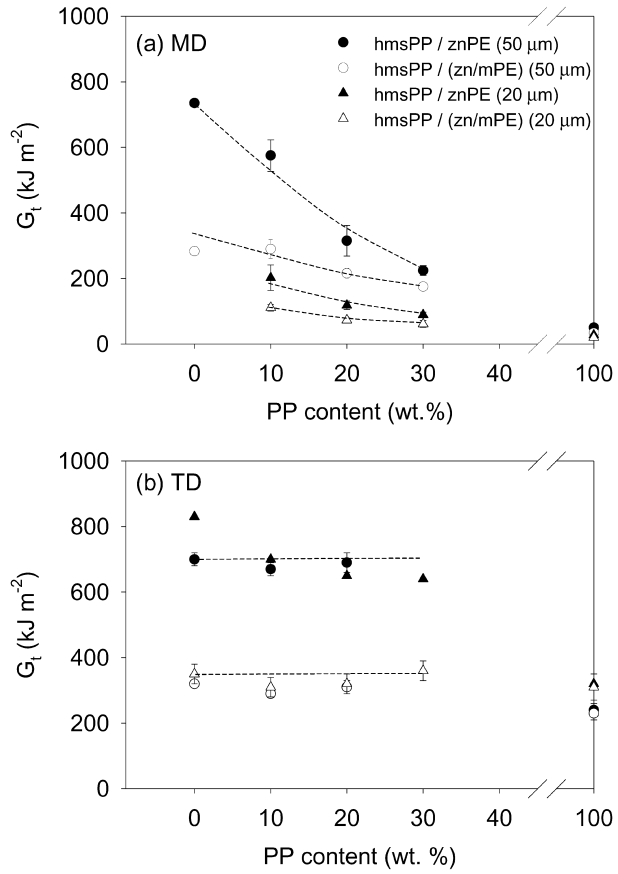

Fig. 1. Effect of hmsPP content on the tear energy of 20 and 50 μm films: (a) MD tear; and (b) TD tear.

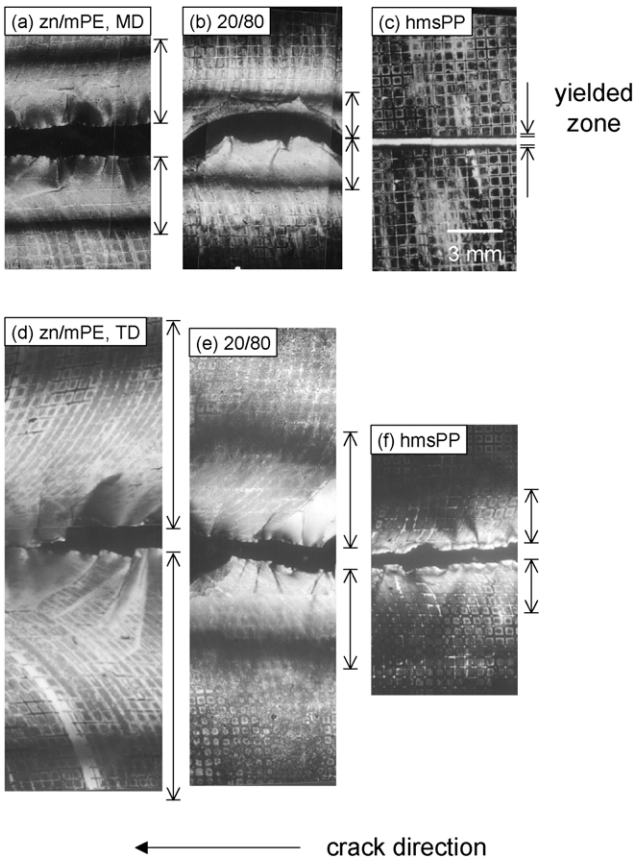

Fig. 2. Polarized light micrographs of torn 50 μm films: (a) MD tear of zn/mPE; (b) MD tear of hmsPP/(zn/mPE) 20/80; (c) MD tear of hmsPP; (d) TD tear of zn/mPE; (e) TD tear of hmsPP/(zn/mPE) 20/80; and (f) TD tear of hmsPP. Arrows indicate the width of the yielded zone.

Examination of the yielded zone between crossed polarizers revealed that squares in the grid pattern had deformed into parallelograms, Fig. 2. The boundary between deformed and undeformed grid squares coincided with the change in interference colors, which was used to define the yielded zone width (W). Increasing the amount of hmsPP in the film decreased W dramatically in MD tear, Table 1. In TD tear, the change in interference colors was not as sharp, the yielded zone was consistently wider than in MD tear, and the width was not as strongly affected by hmsPP content.

The relationship between yielded zone width and MD tear energy is shown in Fig. 3a. The linear correlation was noted previously [7], and was interpreted as a common deformation mechanism irrespective of film thickness, blend composition, or polyethylene type. Furthermore, extrapolation to zero tear energy indicated that the deformation mechanism associated with the yielded zone provided the resistance to tearing in these films. A similar relationship between yielded zone width and TD tear energy was not observed, Fig. 3b. Although the damage zone narrowed as the amount of hmsPP in the film increased, the TD tear energy was largely unaffected by blend composition and depended primarily upon the type of polyethylene.

3.2. Crack-tip damage zone

Examination of the film ahead of the crack tip revealed a triangular damage zone, Fig. 4a. The strain distribution was described by deformation of the grid pattern as shown in Fig. 4b. The squares were highly deformed in the direction of loading whereas the lateral dimension was reduced only to about 80% of the original width due to constraint by the surrounding material. The draw ratio at the crack tip $\lambda_c = L/L_o$ with L_o taken as the original length of the grid squares and L the length of the grid squares at the crack tip was typically about 4 for MD tear, Fig. 5a. In TD tear, λ_c was higher for films with znPE than for films with zn/mPE, Fig. 5b. Also, λ_c decreased slightly with increasing hmsPP content.

To replicate the partially constrained stress state at the MD crack tip, wide film specimens were stretched in the transverse direction perpendicular to the direction of MD crack growth. Stress–strain curves were characterized by yielding, with a maximum in the stress accompanied by formation of a neck, Fig. 6. As the hmsPP content increased, the stress maximum became more pronounced and the neck became noticeably sharper. A plateau of constant stress accompanied propagation of the neck. The plateau

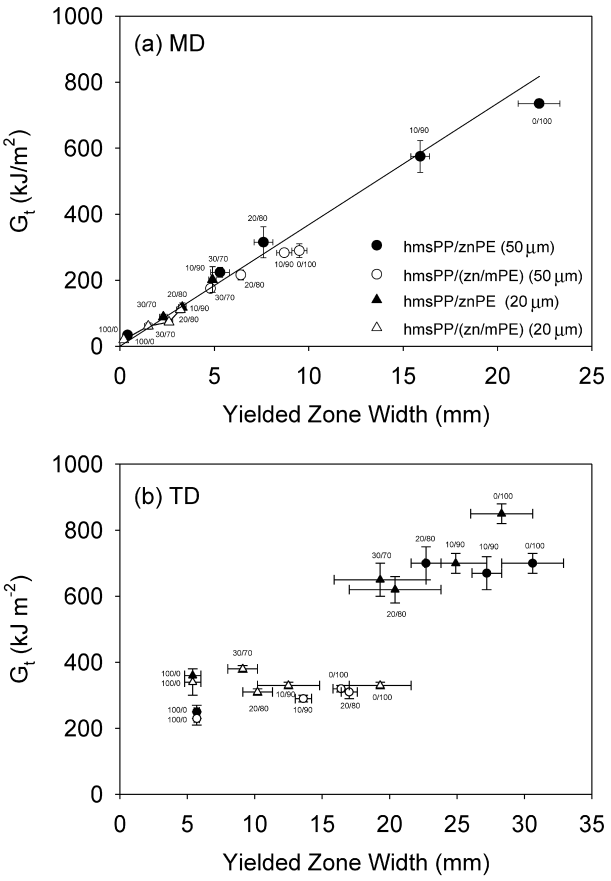

Fig. 3. Relationship between tear energy and yielded zone width: (a) MD tear; and (b) TD tear.

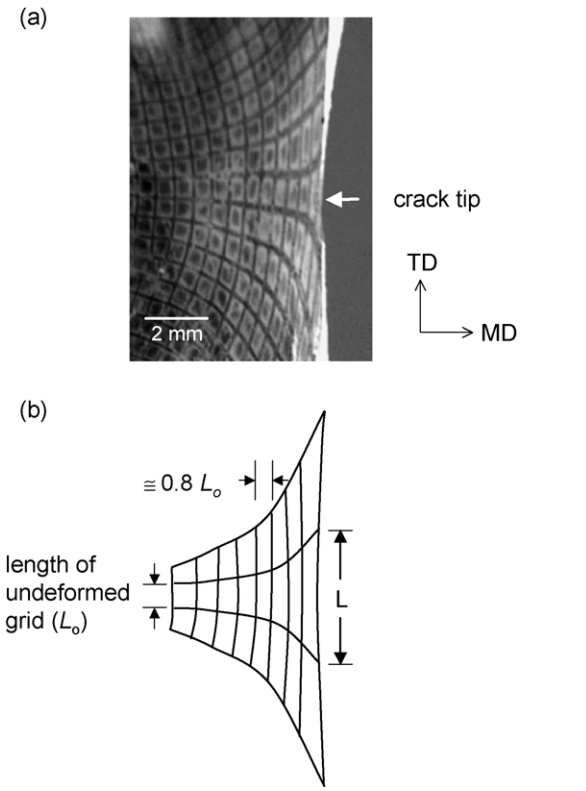

Fig. 4. Crack-tip damage zone: (a) photograph of the damage zone of 20 μm hmsPP/(zn/mPE) 10/90 in MD tear; and (b) schematic representation of the deformed grid pattern.

terminated at the natural draw ratio with a gradual increase in stress to fracture as the film uniformly strain-hardened. In these tests, the lateral draw ratio in the center of the neck was very close to $0.8L_o$, closely reproducing the strain state measured at the crack tip. For comparison, the strain ε_c corresponding to the crack tip draw ratio ($\varepsilon_c = 100(\lambda_c - 1)$) is indicated on each stress–strain curve.

To replicate the partially constrained stress state at the TD crack tip, wide film specimens were stretched in the machine direction perpendicular to the direction of TD crack growth, Fig. 7. The stress–strain curves of znPE and zn/mPE films were almost the same in the transverse and machine directions, consistent with the nearly isotropic lamellar morphology of these films. They exhibited the characteristic double yield with formation of a diffuse neck [15,16]. In contrast, hmsPP film exhibited much higher stresses in the machine direction than in the transverse direction. Moreover, the prominent yield maximum in the transverse direction stress–strain curves was absent in the machine direction. The anisotropic stress–strain response reflected the highly oriented shish-kebab morphology of hmsPP film. The blend films exhibited gradually increasing stress levels as the amount of hmsPP increased. This trend was more evident in the machine direction, due to more effective reinforcement by the elongated hmsPP domains, than in the transverse direction. However, as the hmsPP content increased, the yield maximum did not sharpen in machine direction stress–strain curves. Indeed, the blend films exhibited the characteristic double yield of znPE and zn/mPE films, and the resulting neck was relatively diffuse.

In MD tear, the strain at the crack tip ε_c corresponded on the transverse direction stress–strain curve to the strain at the end of the plateau where the specimen was fully necked and the stress began to increase into the strain-hardening region (Fig. 6). Thus, the crack-tip draw ratio λ_c for MD tear corresponded to the natural draw ratio measured in constrained uniaxial tension for all the 50 and 20 μm films with the exception of 20 μm znPE and zn/mPE films, Table 1. These films drew into the strain-hardening region at the crack tip. This feature was associated with formation of strain-induced fibrillar crystals that caused the crack to curve [7].

In TD tear, λ_c corresponded to the natural draw ratio of zn/mPE film, whereas at the crack tip znPE film extended well beyond the natural draw ratio to the normal fracture strain (Fig. 7). This characteristic carried over to the blend films and was at least partially responsible for the higher TD tear energy to hmsPP/znPE films compared to hmsPP(zn/mPE) films.

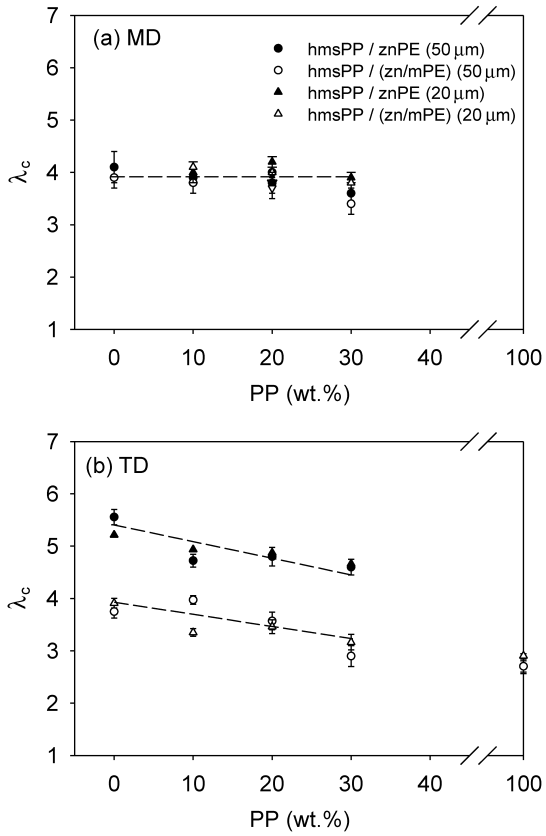

Fig. 5. Effect of hmsPP content on the crack-tip draw ratio of 20 and 50 μm films: (a) MD tear; and (b) TD tear.

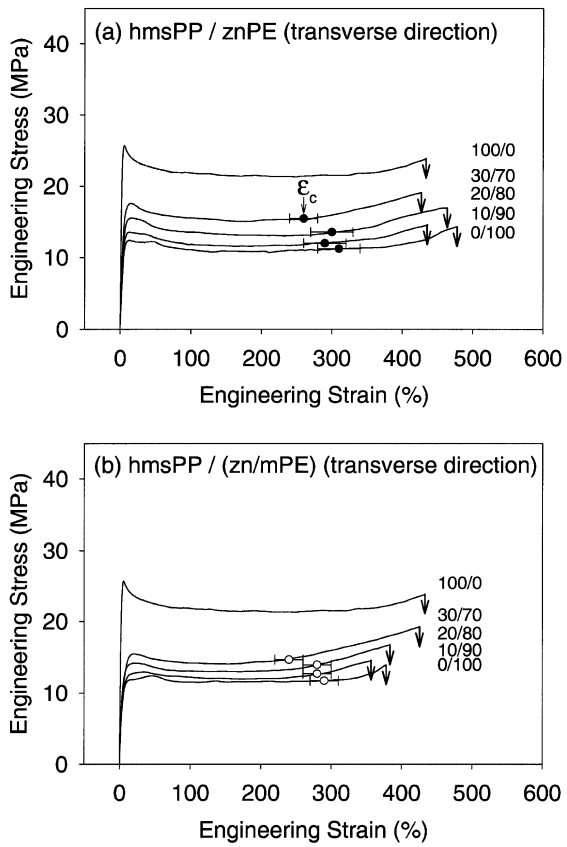

Fig. 6. Constrained stress–strain curves of 50 μm film perpendicular to the MD: (a) hmsPP/znPE films; and (b) hmsPP/(zn/mPE) films. The circle on each curve locates the strain corresponding to the crack-tip draw ratio.

3.3. Mechanism of MD tear

Relationships between certain features of the yielded zone and the measured tear energy that were previously established for MD tear did not hold for TD tear. In particular, TD tear energy was not proportional to yielded zone width (Fig. 3b). Moreover, λ_c in TD tear related differently to film properties measured in constrained uniaxial tension (Fig. 5b). The distinctions between MD and TD tear suggested different deformation mechanisms of the anisotropic film morphology.

Acid etching revealed the morphological features that accompanied the gradually increasing strain through the damage zone approaching the MD crack tip. Deformation of 50 μm hmsPP/znPE 10/90 film is illustrated with a series of AFM phase images in Fig. 8 that shows the undeformed blend morphology ahead of the damage zone, a region approximately midway in the damage zone, and a region immediately adjacent to the crack tip. In these images, the higher modulus hmsPP appears as lighter, thinner lamellae and the lower modulus polyethylene as darker, thicker lamellae. In the undeformed blend, a lighter hmsPP domain, surrounded by the darker PE matrix, extended in the extrusion direction, parallel to the direction of crack propagation, Fig. 8a. The 2.5 μm image shows the hmsPP crystallized in a planar shish-kebab structure consisting of stacked hmsPP lamellae with lamellar long axes perpendicular to the extrusion direction [3]. Near the hmsPP domain, znPE lamellae were oriented with long axes ±40–50° to the extrusion direction. These lamellae produced the herringbone pattern characteristic of epitaxially crystallized polyethylene [17,18]. There was no evidence of an amorphous interfacial layer that prevented epitaxial crystallization of polyethylene in melt blends with hmsPP [3]. In thin film, it was advantageous for mobile amorphous EPR fractions of the impact-modified hmsPP to locate at the film surface rather than at the phase interface [19].

The image in Fig. 8b shows a region approximately midway in the damage zone. Despite the high extension, epitaxially crystallized znPE remained adhered to the hmsPP domains. Remains of the herringbone texture were seen near the hmsPP domain where good adhesion constrained large deformation of the matrix. These regions clearly revealed the znPE yield processes as the lamellae broke up into blocks and reformed as fibrillar structures. Away from the hmsPP domain, the znPE matrix was drawn into fibrillar structures. Good stress transfer resulted in rotation of undeformed hmsPP domains into the loading direction.

At the crack tip, most of the znPE was drawn into a dark, fibrillar texture, Fig. 8c. The PP domains were rotated

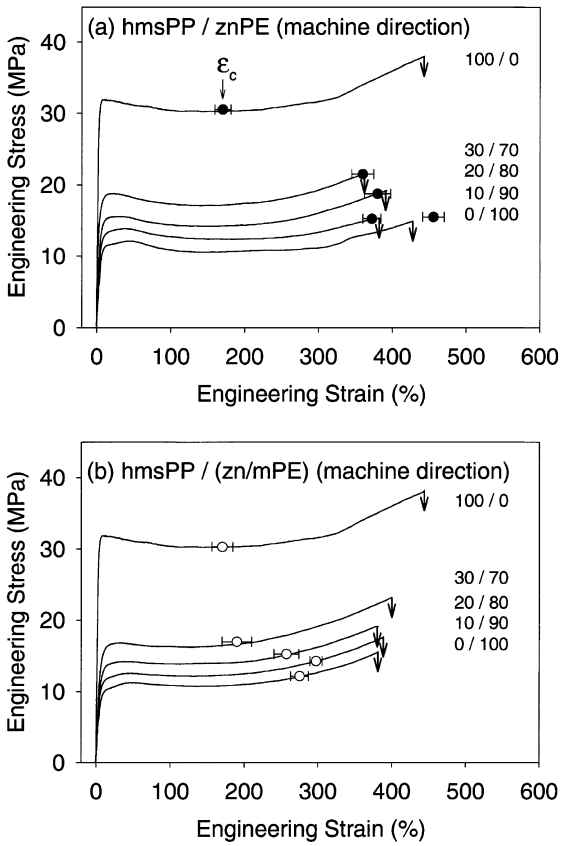

Fig. 7. Constrained stress–strain curves of 50 μm film perpendicular to the TD: (a) hmsPP/znPE films; and (b) hmsPP/(zn/mPE) films. The circle on each curve locates the strain corresponding to the crack-tip draw ratio.

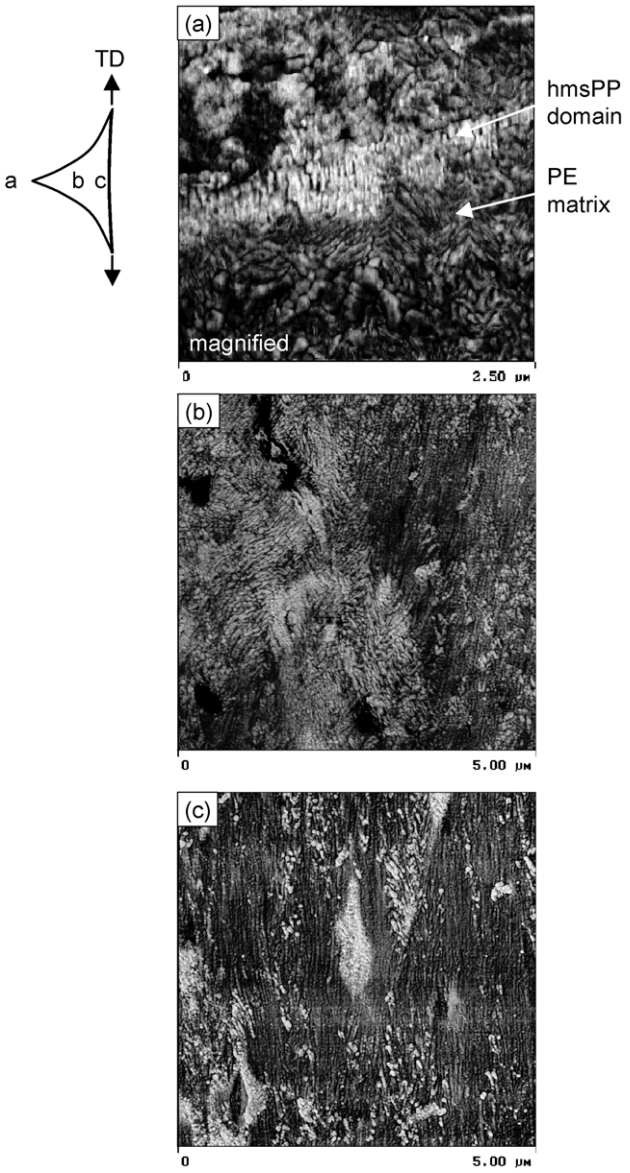

Fig. 8. AFM phase images from the damage zone of 50 μm hmsPP/znPE 10/90 film in MD tear: (a) undeformed film ahead of the damage zone; (b) midway through the damage zone; and (c) at the crack tip.

parallel to the extension direction. Within the hmsPP domains, shear displacement of the lamellar stacks was evident. Shearing of the hmsPP domains was only observed within 0.5 mm of the crack tip, and thus occurred in the last stages of draw before the crack propagated through the damage zone.

Deformation processes that occur in the damage zone during MD tear are summarized in Fig. 9. Deformation of the anisotropic structure begins by breakup of polyethylene lamellae that are not close to an hmsPP domain. The lamellar blocks resemble a beaded string texture that appears increasingly fibrillar as the strain increases closer to the crack tip. The strain gradient causes rotation of hmsPP domains into the loading direction and in a later stage causes shear displacement of reoriented hmsPP lamellae. Although they may be somewhat elongated from their original shape close to the crack tip, hmsPP domains remain largely intact. Throughout the deformation process, there is no indication of interfacial failure. As a consequence of exceptionally good adhesion between epitaxially crystallized polyethylene and polypropylene [20,21], hmsPP domains in blend films constrain deformation of nearby polyethylene lamellae. Even at the crack tip, where fracture is imminent, some partially deformed polyethylene lamellae retain evidence of the herringbone texture of epitaxially crystallized polyethylene.

Structural modifications, such as increasing the number of hmsPP domains or increasing the aspect ratio of hmsPP domains by using a higher take-off rate to decrease film thickness [3], increase constraint on deformation of the polyethylene matrix and make it harder for hmsPP domains to rotate into the loading direction. It is not surprising that structural factors that increase constraint on the polyethylene matrix also reduce MD tear energy. However, as pointed out here and elsewhere [7], increased constraint does not necessarily result in a lower draw ratio at the crack tip, at least not enough lower to account for the reduction in tear energy. The key factor is the amount of deformed material, which is determined by the strain gradient in the

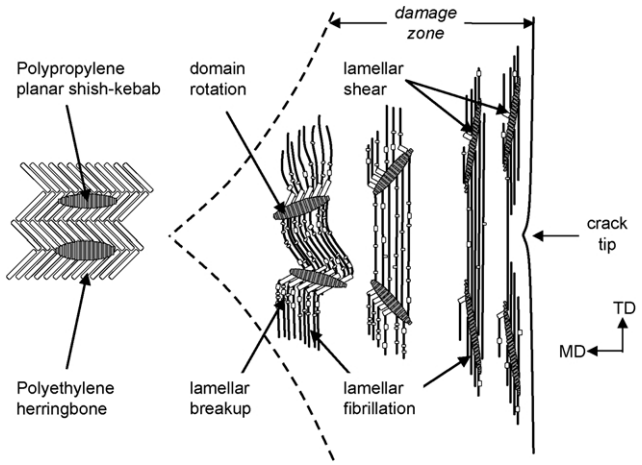

Fig. 9. Schematic illustration of the deformation processes in the damage zone of hmsPP blend films during MD tear. Polypropylene lamellae of the shish-kabob structure are represented as aligned rectangles in the dark domains, epitaxially crystallized polyethylene lamellae of the matrix are represented as rectangles arranged in a herringbone pattern.

damage zone. Constitutive behavior related to yielding and necking determines the strain distribution at the crack tip. It can be speculated that a sharper neck localizes yielding to a smaller region. In this regard, the tendency of hmsPP to sharpen the broad yield and diffuse neck that characterize polyethylene films may be directly related to the smaller damage zone and lower MD tear energy.

3.4. Mechanism of TD tear

The damage zone ahead of the TD tear crack in 50 μm hmsPP/znPE 10/90 film is shown in the series of AFM images in Fig. 10. In this configuration, loading was in the direction of extrusion, parallel to the long axes of the elongated PP domains, Fig. 10a. Approximately midway through the damage zone, breakup of polyethylene lamellae appeared everywhere on the image, not preferentially away from the hmsPP domains, Fig. 10b. In the TD tear orientation, hmsPP domains did not constrain polyethylene lamellae to the extent they did in MD tear. Breakup of epitaxially crystallized polyethylene lamellae was facilitated by shear displacement of hmsPP lamellae. Orientation of the hmsPP shish-kebab with the lamellar long axis perpendicular to the direction of loading facilitated slip along crystallographic planes and between lamellar blocks. At the crack tip, shear deformation of hmsPP domains resulted in considerable elongation over the original shape, Fig. 10c. The polyethylene matrix was almost entirely fibrillated. Dark streaks indicated possible splitting of the fibrillar texture. This contrasted to the crack tip in MD tear where constraint imposed by the hmsPP domains prevented such a high degree of polyethylene fibrillation (cf. Fig. 8c).

Deformation during TD tear is schematically illustrated in Fig. 11. As a consequence of approximately 40–50° orientation of epitaxially crystallized znPE lamellae and low degree of orientation of non-epitaxially crystallized lamellae, deformation of the znPE matrix occurs in essentially the same way in TD and MD tear with sequential breakup into lamellar blocks, reassembly into beaded strings, and transformation into fibrillar structures. The primary difference between TD and MD tear is the orientation of hmsPP domains. With their long axes perpendicular to the loading direction hmsPP lamellae are vulnerable to shear deformation. This relieves constraint on epitaxially crystallized znPE lamellae and permits the znPE matrix to deform more uniformly than in MD tear. Close to the crack tip, znPE lamellae are almost completely fibrillated and the hmsPP domains are highly extended from their original shape as a result of lamellar shear processes.

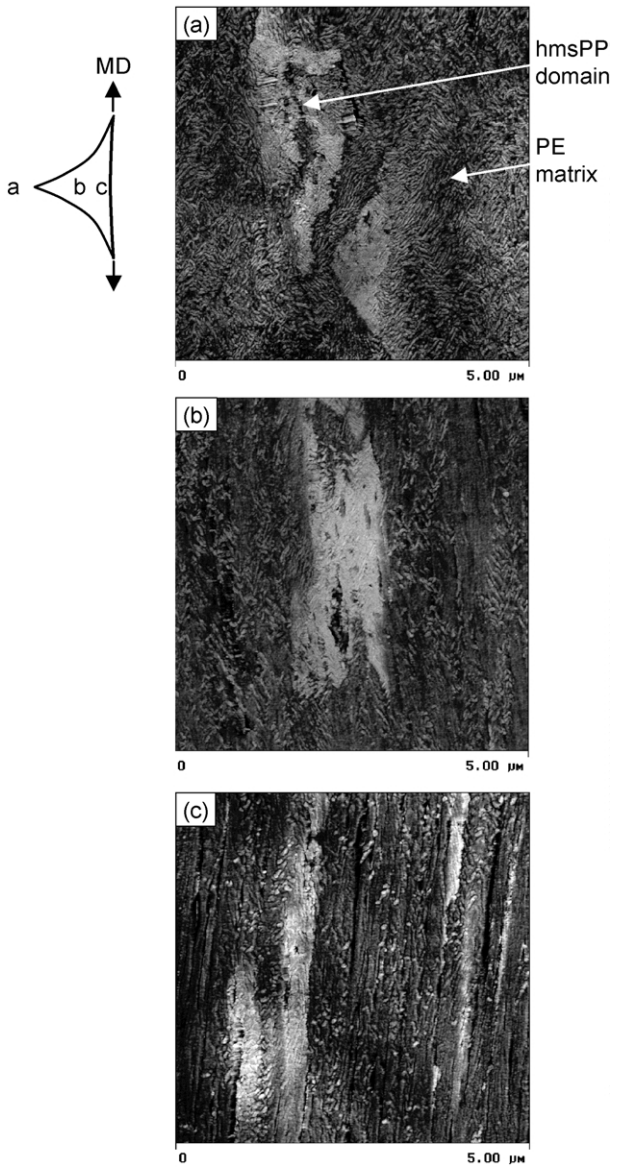

Fig. 10. AFM phase images from the damage zone of 50 μm hmsPP/znPE 10/90 film in TD tear: (a) undeformed film ahead of the damage zone; (b) midway through the damage zone; and (c) at the crack tip.

Higher extension at the crack tip of 50 μm znPE/hmsPP 10/90 in TD tear compared to MD tear, which is inferred

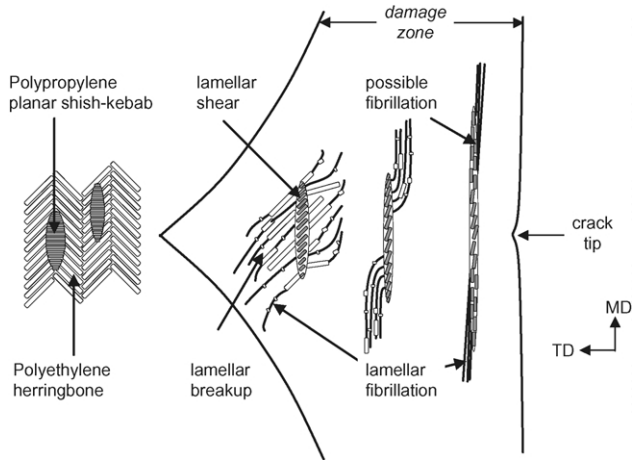

Fig. 11. Schematic illustration of the deformation processes in the damage zone of hmsPP blend films during TD tear. Polypropylene lamellae of the shish-kabob structure are represented as aligned rectangles in the dark domains, epitaxially crystallized polyethylene lamellae of the matrix are represented as rectangles arranged in a herringbone pattern.

from the AFM images (Figs. 8c and 10c), is confirmed by the larger crack tip draw ratio measured in TD tear ($\lambda_c = 4.7$) compared to MD tear ($\lambda_c = 3.9$). In relationship to the stress–strain curve, the difference in λ_c corresponds to a change from fracture at the normal fracture strain in TD tear to fracture at the natural draw ratio in MD tear. Local stress concentrations imposed by reorientation of hmsPP domains into the loading direction in MD tear may have acted as flaws thereby reducing the fracture strain.

3.5. Yielded zone

The process of stable crack propagation transformed the triangular damage zone at the crack tip into a continuous yielded zone of constant width. At the point of fracture, only the material in a small area directly ahead of the crack achieved full draw, as indicated by the strain gradient in photographs of the crack tip. As the fractured edges separated, further extension of the surrounding material created the yielded zone of 50 μm hmsPP/(zn/mPE) 10/90 shown in Fig. 12a. Closely spaced color changes in the interference pattern of MD tears (cf. also Fig. 2a and b) suggested a sharp boundary between yielded and unyielded material. Uniform deformation of the grid squares across the width of the damage zone indicated that the yielded material was drawn to a characteristic draw ratio. An AFM image from the sharp boundary between yielded and unyielded material shows the beginning stage of zn/mPE lamellar breakup with the hmsPP domains retaining their original orientation perpendicular to the loading direction, Fig. 12b. An image of the yielded zone shows broken-up zn/mPE lamellae close to an hmsPP domain, Fig. 12c. The hmsPP lamellae are somewhat sheared. Away from the hmsPP domain the zn/mPE lamellae are fully extended into fibril structures. These features, which characterized the entire yielded zone, closely resembled the most highly deformed

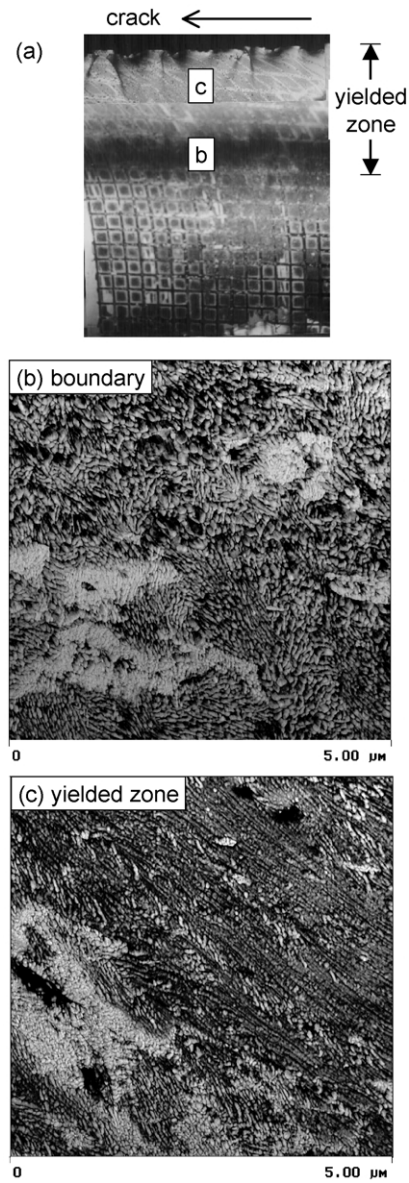

Fig. 12. The yielded zone of 50 μm hmsPP/(zn/mPE) 10/90 film in MD tear: (a) the yielded zone; (b) AFM phase image from a region near the boundary of the yielded zone; and (c) AFM phase image from a region midway through the yielded zone.

region of the damage zone at the crack tip (compare with Fig. 8c). Stress redistribution in the trouser legs after fracture produced a complex strain response with a component parallel to the tear direction. Reorientation of the fibrillar texture in Fig. 12b was a result of this shear field.

The yielded zone was wider in TD tear than MD tear (cf. Fig. 2). More gradual color changes in the interference pattern suggested that yielding was more diffuse in TD tear. The broad strain gradient associated with diffuse yielding was apparent in the deformation of grid squares through the yielded zone of 50 μm hmsPP/znPE 10/90 in Fig. 13a. An AFM image from the diffuse boundary region shows the initial stages of lamellar deformation with break up of znPE lamellae into blocks and shearing of hmsPP domains,

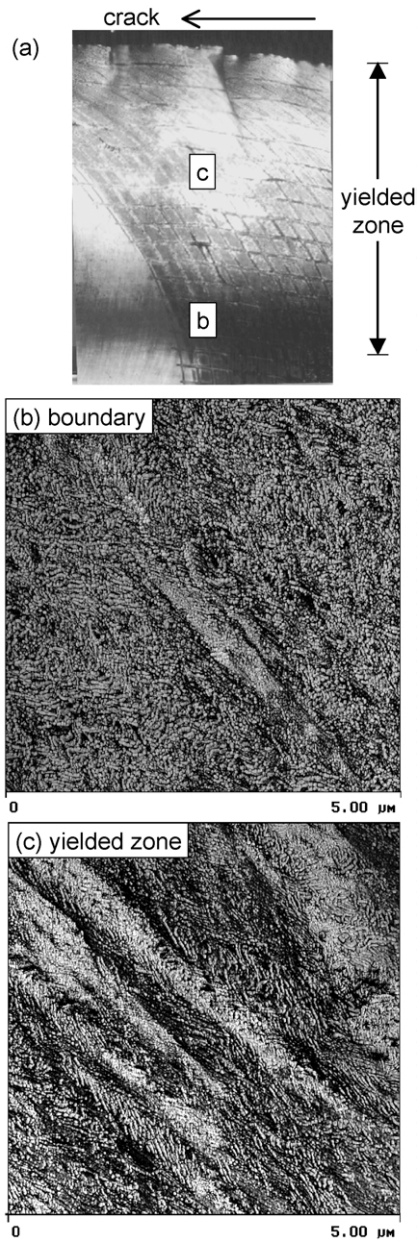

Fig. 13. The yielded zone of 50 μm hmsPP/znPE 10/90 film in TD tear: (a) the yielded zone; (b) AFM phase image from a region near the boundary of the yielded zone; and (c) AFM phase image from a region midway through the yielded zone.

Fig. 13b. An AFM image from midway in the yielded zone shows more breakup znPE lamellae and, in places, the beginning of fibrillar structures, Fig. 13c. However, the highly drawn fibrillar morphology at the crack tip is not apparent at this position in the yielded zone (compare with Fig. 10c). The morphological features are consistent with a gradual yielding process that produces a gradient in the amount of deformation through the width of the yielded zone. It can be imagined that the highly drawn fibrillar structure seen at the crack tip is only achieved close to the fractured edge. Stress redistribution in the trouser legs caused the hmsPP domains in Fig. 13b and c to rotate into shear direction.

It is now possible to understand why MD tear energy correlates with the width of the damage zone, but TD tear energy does not. Material in the MD yielded zone was uniformly drawn to a strain close to λ_c. The value of λ_c did not depend strongly on composition being close to 4 for all films. Instead, MD tear energy correlated with the amount of material that was drawn into the yielded zone. This permitted a quantitative calculation of tear energy from the stress–strain relationship by assuming that all the material in the yielded zone was drawn to λ_c [7]. Because yielding in TD tear was much more diffuse, strain in the yielded zone could not be considered as constant and equal to λ_c. Although more material was drawn into the yielded zone in TD tear than in MD tear, not all the material was drawn to λ_c. It would be necessary to consider both the amount of material in the yielded zone and the strain gradient in order to estimate tear energy from the stress–strain relationship.

3.6. Deformation of hmsPP

In contrast to the plastic deformation and yielding of films with znPE or zn/mPE, MD tear of hmsPP film created only a small stress-whitened zone, Fig. 14. The undeformed film in Fig. 14a exhibited the shish-kebab morphology described previously [3]. In the stress-whitened zone, the shish-kebabs remained undeformed, Fig. 14b. Numerous dark streaks were verified from height images to be microcracks. Cracking between shish-kebabs in the direction perpendicular to the load suggested weak interconnections between neighboring shish-kebabs.

Microcracking was not observed in the blends, either within hmsPP domains or between hmsPP domains and the polyethylene matrix. It can be hypothesized that microcracking was inhibited in blend films by the small domain size, possibly as small as a single shish-kebab, and good adhesion between hmsPP and the matrix [20,21]. These factors promoted rotation of hmsPP domains (MD tear) and shear of hmsPP lamellae (MD and TD tear) during yielding instead of microcracking.

The significance of hmsPP shear processes can be tested by examining the tear behavior at temperatures below the glass transition temperature of hmsPP at approximately 0 °C. It can be imagined that decreasing the temperature should markedly affect lamellar shear processes, which depend on the mobility of the amorphous component. In addition to the contribution that lamellar shear per se makes to the tear energy, the degree to which shear deformation of hmsPP domains relieves constraint and permits the surrounding polyethylene matrix to yield can have a large impact on tear energy.

Effects of hmsPP content on MD and TD tear of znPE films at 20 and − 10 °C are compared in Table 2. At −10 °C, znPE film retained high tear resistance with balanced MD

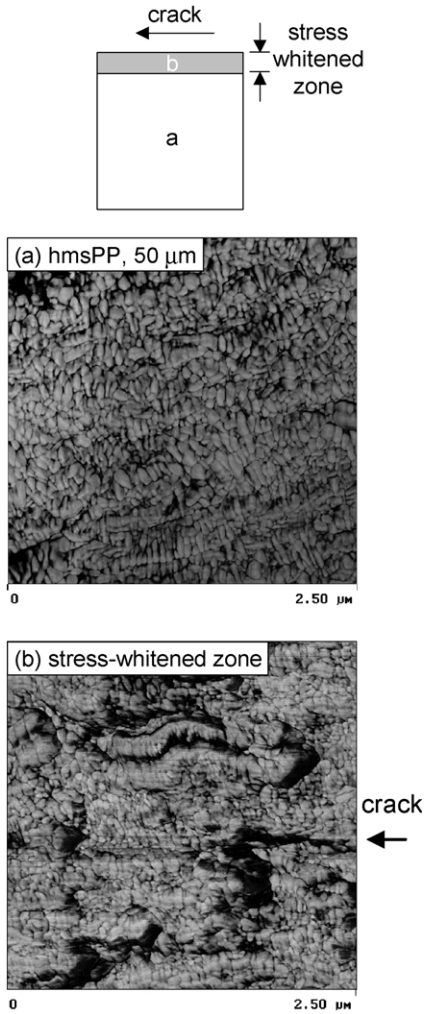

Fig. 14. AFM phase images from the stress-whitened zone of 50 μm hmsPP film in MD tear: (a) outside the yielded zone; and (b) within the stress-whitened zone.

and TD performance. In blends, the −10 °C MD tear resistance decreased with increasing hmsPP content paralleling the results at 20 °C, except that the −10 °C values were 30–50% lower, Fig. 15a. The decrease in MD tear arises from constraints on matrix deformation imposed by hmsPP domains as they are forced to rotate into the loading direction. This aspect does not assume deformation of hmsPP and therefore the functional relationship between tear energy and hmsPP content is not affected by the glass transition of hmsPP. However, decreasing the temperature below the glass transition suppresses hmsPP lamellar shear processes that occur in the last stage of MD tear. This reduces the draw ratio at the tear crack tip and accordingly the tear energy at −10 °C is systematically lower than at 20 °C.

In TD tear at 20 °C, shear deformation of the hmsPP domains accompanied all stages of deformation and indeed permitted the polyethylene matrix to achieve a very high draw ratio at the crack tip. The effect of inhibiting shear deformation of the hmsPP domains was dramatic, Fig. 15b.

Table 2
Effect of temperature on tear energy

Material	hmsPP (wt%)	MD		TD	
		20 °C	−10 °C	20 °C	−10 °C
50 μm films					
hmsPP/znPE	0	740 ± 30	>800	700 ± 20	>800
	10	580 ± 50	370 ± 30	670 ± 20	550 ± 70
	20	320 ± 50	240 ± 20	690 ± 30	410 ± 10
	30	220 ± 20	130 ± 20	‡	‡
hmsPP/(zn/mPE)	0	280 ± 10	290 ± 10	320 ± 10	390 ± 10
	10	290 ± 30	190 ± 20	290 ± 10	290 ± 30
	20	220 ± 20	130 ± 10	310 ± 20	270 ± 30
	30	180 ± 10	110 ± 10	‡	‡
hmsPP	100	34 ± 3	18 ± 2	230 ± 20	30 ± 3
20 μm films					
hmsPP/znPE	0	‡	‡	830 ± 40	>1000
	10	210 ± 40	120 ± 10	700 ± 30	730 ± 30
	20	120 ± 10	68 ± 6	650 ± 40	540 ± 40
	30	90 ± 10	52 ± 5	640 ± 50	380 ± 40
hmsPP/(zn/mPE)	0	‡	140 ± 10	350 ± 10	430 ± 10
	10	110 ± 10	100 ± 10	310 ± 10	330 ± 20
	20	70 ± 10	64 ± 7	320 ± 10	290 ± 20
	30	60 ± 10	50 ± 10	360 ± 10	250 ± 20
hmsPP	100	20 ± 3	14 ± 4	310 ± 40	36 ± 7

‡ represents curved crack path.

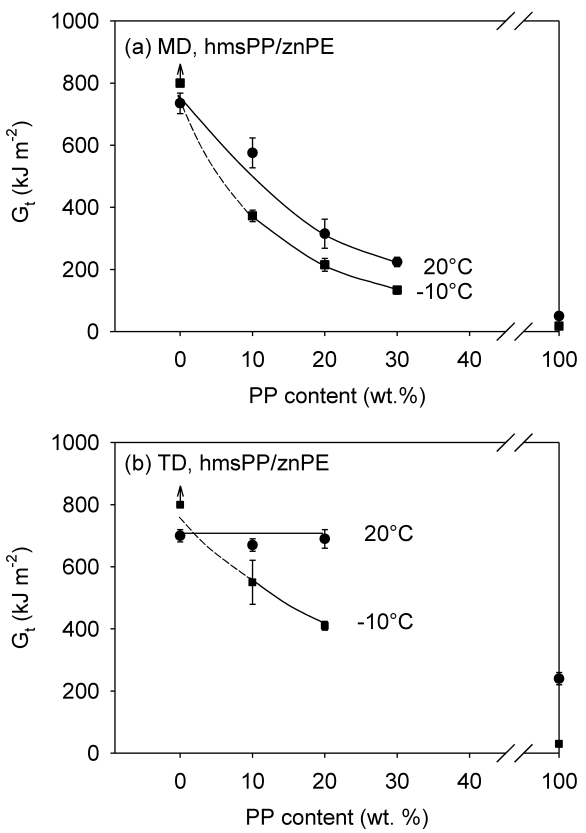

Fig. 15. Effect of temperature on the tear energy of 50 μm znPE, hmsPP/znPE and hmsPP films: (a) MD tear; and (b) TD tear.

It is speculated that at −10 °C, rigid hmsPP domains constrain deformation of the polyethylene matrix, and the tear strength decreases sharply with increasing hmsPP content.

4. Conclusions

Yielding in the vicinity of the propagating crack provided the tear resistance of polyethylene blown film. The balanced yield characteristics of polyethylene film reflected the nearly isotropic lamellar morphology. In contrast, the highly oriented shish-kebab morphology of blown hmsPP films resulted in anisotropic behavior. Because domains of hmsPP retained the oriented shish-kebab morphology in blend films the yield characteristics became increasingly anisotropic as the amount of hmsPP in the blend increased to 30 wt%. The most important manifestation was a significant reduction in MD tear.

Probing the plastic deformation mechanisms of ductile tearing at the lamellar size scale provided insight into the anisotropic behavior. Good adhesion of polyethylene and hmsPP in blend films prevented interfacial failure and provided stress transfer to the dispersed domains at high strains. If the hmsPP shish-kebab was aligned in the loading direction, orientation of lamellar long axes perpendicular to loading facilitated shear deformation along weak crystallographic planes or between lamellar blocks. This enabled the hmsPP domains to deform concurrently with lamellar breakup and fibrillation of the polyethylene matrix. As a result, the blend film retained diffuse yielding in tensile stress–strain curves and preserved good resistance to propagation of a TD tear crack. Indeed, TD tear energy of blend films depended more on the type of polyethylene than on the amount of hmsPP in the blend or on the aspect ratio of the hmsPP domains (i.e. film thickness).

Alignment of the hmsPP shish-kebab perpendicular to the loading direction had a different and deleterious effect. In tear tests of hmsPP films, the presence of a stress concentration acting parallel to the shish-kebab produced microcracks along weak boundaries between shish-kebabs, which resulted in very poor MD tear resistance. In blend films, good dispersion of the hmsPP phase and good adhesion to the polyethylene matrix enabled other deformation mechanisms to replace cavitation of hmsPP. Extension of the polyethylene matrix by the normal processes of lamellar breakup and fibrillation caused rotation of hmsPP domains into the loading direction and in a later stage shear displacement of reoriented hmsPP lamellae. There was no evidence of interfacial failure. Instead, hmsPP domains locally constrained deformation of the polyethylene matrix. Increasing the amount of hmsPP or increasing the aspect ratio of hmsPP domains increased constraint on the polyethylene. This was manifest in tensile stress–strain curves as sharper yielding. Factors that increased constraint on the polyethylene matrix also reduced the resistance to propagation of an MD tear crack.

Acknowledgements

The generous technical and financial support of The Dow Chemical Company is gratefully acknowledged.

References

[1] Hoenig WD, Bosnyak CP, Sehanobish K, Van Volkenburgh W, Ruiz C, Tau LM. Proc SPE ANTEC 2000;1843–6.
[2] Wu S, Bosnyak CP, Sehanobish K, Van Volkenburgh W, Ruiz C, Tau LM. Proc SPE ANTEC 2001;2828–32.
[3] Chang AC, Tau L, Hiltner A, Baer E. Polymer 2002; 43:4923–33.
[4] Gross B, Petermann J. J Mater Sci 1984;19:105–12.
[5] Gohil RM. J Polym Sci: Polym Phys Ed 1985;23:1713–22.
[6] Jaballah A, Rieck U, Petermann J. J Mater Sci 1990;25:3105–10.
[7] Chang AC, Tau L, Hiltner A, Baer E. Polym Engng Sci 2002; in press.
[8] Peterlin A. J Mater Sci 1971;6:490–508.
[9] Keller A, Pope DP. J Mater Sci 1971;6:453–78.
[10] Galeski A, Bartczak Z, Argon AS, Cohen RE. Macromolecules 1992; 25:5705–18.
[11] Bartczak Z, Argon AS, Cohen RE. Polymer 1994;35:3427–41.
[12] Hiss R, Hobeika S, Lynn C, Strobl G. Macromolecules 1999;32: 4390–403.
[13] Sabbagh AB, Lesser AJ. J Polym Sci, Part B: Polym Phys 1999;37: 2651–63.
[14] Olley RH, Bassett DC. Polymer 1982;23:1707–10.
[15] Seguela R, Rietsch F. J Mater Sci Lett 1990;9:46–7.
[16] Brooks NW, Duckett RA, Ward IM. Polymer 1992;33:1872–80.
[17] Lotz B, Wittman JC. J Polym Sci, Part B: Polym Phys 1987;25: 1079–87.
[18] Wittman JC, Lotz B. Prog Polym Sci 1990;15:909–48.
[19] Chang AC, Chum SP, Hiltner A, Baer E. J Appl Polym Sci 2002; in press.
[20] Peterman J, Broza G, Rieck U, Kawaguchi A. J Mater Sci 1987;22: 1477–81.
[21] Lee IH, Schultz JM. J Mater Sci 1988;23:4237–43.